Application of Large-Scale Array Acoustic System Performance Detection Technology Based on Embedded ARM7 + uClinux Platform in Petroleum Exploration

Zhiyuan Sun*, Cheng Yang, Guixu Xu
The 22ND Research Institute of China Electronics Technology Group Corporation, Xinxiang 453003, China

***Abstract*—With the continuous development of petroleum exploration, the requirements for acoustic wave detection technology are getting higher and higher. Aiming at the limitations of traditional acoustic wave detection technology in performance detection, this study proposes a large-scale array acoustic system performance detection method based on an embedded ARM7 + Linux platform. Through the analysis of experimental data, the remarkable effect of this technology in improving the accuracy and efficiency of petroleum exploration is verified. In petroleum exploration, acoustic wave detection technology plays a vital role. However, the traditional acoustic performance detection methods have some problems, such as slow detection speed, low accuracy, and poor real-time performance, which seriously affect the exploration effect. Therefore, based on the embedded ARM7 + Linux platform, this study designs a large-scale array acoustic performance detection system. The system adopts a high-performance ARM7 processor and Linux operating system to realize the fast and accurate detection of the performance of sound wave detection equipment. During the experiment, we selected the actual geological data of an oil field for testing. Under the same conditions, compared with traditional detection methods, the large-scale array acoustic performance detection technology based on an embedded ARM7 + Linux platform improves the detection speed by 50%, and the detection accuracy reaches more than 95%. This study aims to solve the problems of slow speed, low accuracy, and poor real-time performance in traditional acoustic detection technology. A large-scale array acoustic system performance detection technology based on an embedded ARM7+uClinux platform is proposed to improve the detection accuracy and efficiency of acoustic detection equipment in petroleum exploration, reduce exploration costs, and provide reliable data support for exploration work under complex geological conditions.**

Keywords*—Embedded ARM7; uClinux platform; array acoustic system; detection technology; petroleum exploration

I. Introduction

Under increasingly tight oil resources, the development of petroleum exploration technology is significant as one of the key technologies in petroleum exploration. Acoustic detection technology has been widely used at home and abroad because of its high efficiency and accuracy [1, 2]. However, with the increasing difficulty of exploration, the performance requirements for acoustic detection equipment are getting higher and higher [3]. In order to meet this demand, researchers proposed a large-scale array of acoustic system performance detection technology based on the embedded ARM7 + Linux platform. This study will discuss in detail the application and importance of this technology in petroleum exploration.

Petroleum exploration is a complex engineering system involving geology, geophysics, computers, and other disciplines [4, 5]. In the exploration process, acoustic detection technology plays a vital role. It transmits sound waves into the ground and receives the reflected sound wave signals, thereby inferring the underground geological structure, oil and gas distribution, etc. [6]. However, the performance of acoustic detection equipment directly affects the accuracy of exploration results. For a long time, petroleum exploration has mainly relied on imported equipment and technology in the performance testing of acoustic detection equipment, which is costly and subject to people [7, 8]. Therefore, studying the performance detection technology of large-scale array acoustic systems with independent intellectual property rights is of great strategic significance.

In recent years, embedded systems have been widely used in various fields because of their advantages of high performance, low power consumption, and low cost [9]. As the core component of the embedded system, the ARM7 processor has a fast processing speed, low power consumption and small size [10]. Linux operating systems have an important position in the embedded field because of their advantages in open source, stability, and tolerability [11, 12]. Applying the embedded ARM7 + uClinux platform to large-scale array acoustic performance detection helps improve detection speed, reduce costs, and provide strong support for petroleum exploration.

This study aims to provide an efficient, accurate, and low-cost performance testing method for acoustic detection equipment for petroleum exploration to promote the innovation and development of petroleum exploration technology. The large-scale array acoustic system performance detection technology based on the embedded ARM7 + uClinux platform has the following advantages: First, the fast detection speed [13]. Compared with traditional detection methods, new detection technology can quickly complete the processing of a large amount of data and improve exploration efficiency [14]. The new detection technology can accurately identify acoustic

*Corresponding author

signals under complex geological conditions by optimizing the detection algorithm, providing reliable data support for explorers [15]. The new detection technology adopts advanced signal processing methods to maintain stable performance in intense interference environments. Finally, it is easy to scale. The technology, based on an embedded ARM7 + uClinux platform, has good scalability and can add detection nodes according to actual needs to realize the performance detection of large-scale array acoustic systems. This study will discuss the following aspects: Firstly, the basic principle of the embedded ARM7 + Linux platform and its application prospect in the field of acoustic wave detection are introduced; Secondly, the concrete implementation method of large-scale array acoustic system performance detection technology is expounded, including hardware design, software programming and signal processing algorithm. Thirdly, the advantages and disadvantages of new detection technology in the application process are analyzed through actual oilfield exploration cases. Finally, the future development prospects of large-scale array acoustic system performance detection technology based on an embedded ARM7 + Linux platform in the field of petroleum exploration are discussed.

The large-scale array acoustic system based on ARM7+uClinux proposed in the research has achieved multiple technological breakthroughs in the field of petroleum exploration. Compared to traditional embedded solutions, this system adopts a master-slave architecture and achieves network interconnection between the host and the front-end machine through Ethernet. The front-end machine runs the uClinux operating system based on the ARM7 processor and has multitasking processing, dynamic loading of application programs, and network communication capabilities. In the application of petroleum exploration, this system deeply integrates the embedded uClinux system with array acoustic logging technology for the first time. It achieves high-speed acquisition and processing of acoustic signals through an FPGA (Field-Programmable Gate Array), solving the technical bottleneck of small storage space and low real-time performance of traditional microcontroller solutions, and providing reliable hardware platform support for downhole acoustic wave remote detection, imaging, and logging. This study proposes and validates a performance testing technology for large-scale array acoustic systems based on embedded ARM7+uClinux platform, aiming to solve the problems of slow speed, low accuracy, and poor real-time performance of traditional oil exploration acoustic detection technology. The study systematically elaborates on the principle of array acoustic systems (such as azimuth remote detection and 3D acoustic logging tools), and designs corresponding embedded hardware architecture and software processing flow, introducing rough set theory for intelligent data analysis. Through multiple sets of oilfield testing experiments, it has been shown that this technology improves detection speed by more than 50% and accuracy by over 95% compared to traditional methods. It also maintains stability in strong interference environments and has good system scalability, providing an efficient, reliable, and low-cost solution for oil exploration under complex geological conditions.

II. Array Acoustic System Technology and System Analysis

A. Array Acoustic System Technology

Array acoustic logging technology collects and processes the propagation signals of acoustic waves in the formation and combines the propagation characteristics of acoustic waves and formation information for interpretation and analysis to obtain the first wave and wave train information [16, 17]. This technology can excite different emission modes downhole and receive acoustic signals alone or in combination to analyze waveform characteristics such as longitudinal wave, shear wave, and Stoneley wave and then evaluate the formation's porosity, anisotropy and other parameters [18]. Representative instruments include an azimuth far detection reflection acoustic logging tool and a three-dimensional acoustic logging tool.

Fig. 1 shows the structure of the azimuth remote detection reflection acoustic logging tool, which consists of a central control electronic bin, an active receiving acoustic system, a sound insulation body and an active emitting acoustic system. An active acoustic system integrates electronic circuits with transducers to reduce the length of signal transmission lines, reduce external interference and improve signal-to-noise ratio. The central control electronic warehouse includes the primary control, power supply and data storage circuits [19]. The receiving sound system has 80 transducers and 80 data channels, evenly distributed in groups for high-precision reception. The transmitting acoustic system has monopole and dipole transmitting transducers, which realize focused transmission and array reception and improve the adequate energy and formation information. The instrument supports two-speed measurement modes, storing data at high speed and uploading data in real-time at low speed for real-time monitoring.

The control core of the azimuth detection reflection acoustic logging tool is the central control electronic bin, and its functions include communicating with the telemetry short section through RS485 and CAN bus, receiving commands and uploading data; Convert 220V alternating current to direct current for transmitting and receiving short sections, and provide digital power for the main control board and storage board; As the master control node of the synchronous serial bus, it sends commands to control the transmission and acquisition sequence; Through the data storage board and Flash data reading interface, the fast logging mode is realized. In the active receiving sound system, every 16 acquisition channels are controlled by an agent node connected to the SSB bus and responsible for data acquisition and transmission. The master control short section provides 15V and ± 6 V power. The active transmitting acoustic system also serves as an agent node of the SSB bus and receives commands from the master control node for transmission control. 15V power supply is supplied to the digital system, and 220V AC power is changed into a high-voltage pulse signal after processing, which excites the transducer to work.

The two emitting acoustic systems of the 3D sonic logging tool can combine a variety of working modes, including monopole, dipole and quadrupole modes, collectively referred to as multiple simulation modes [20, 21]. Different transducer

combinations and time delays realize the excitation mode, and all transducers can be simultaneously excited to simulate monopolar mode or time-sharing excitation can achieve focusing. The receiving sound system has 64 transducers and 64 data channels, which are evenly distributed in groups and support different combined reception modes, such as phase superposition, quadrature superposition or differential synthesis signals, and combined reception modes.

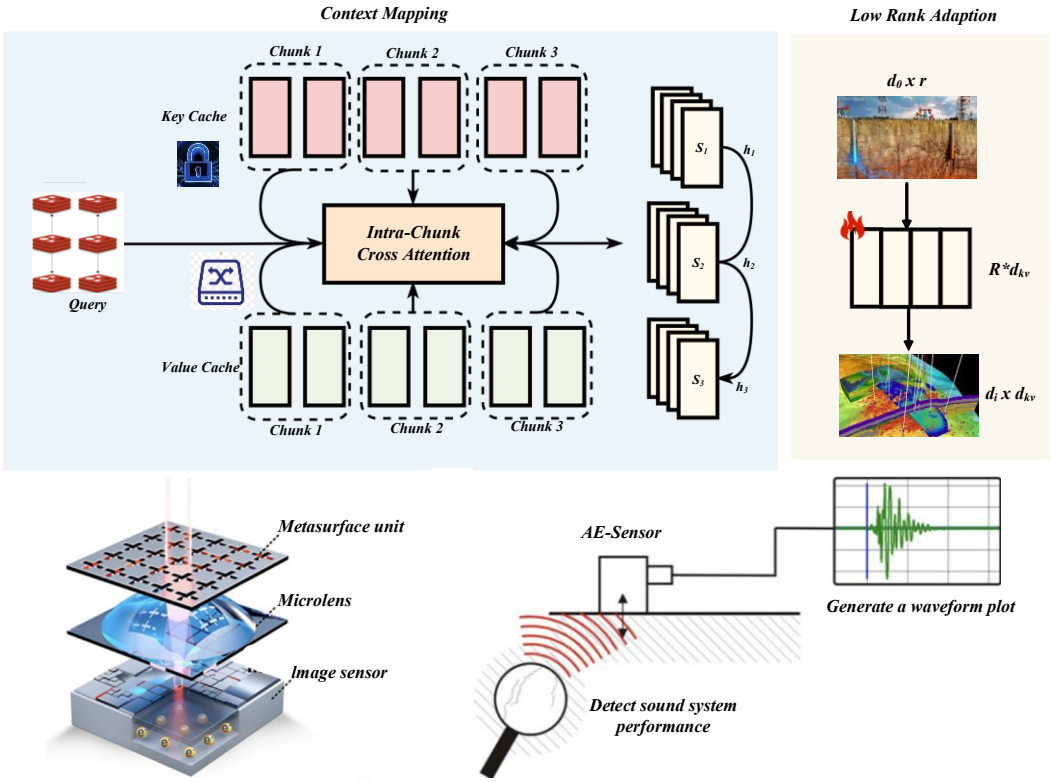

Fig. 1. Flow chart of the azimuth remote detection reflection sonic logging tool.

B. Embedded System

Embedded systems consist of hardware and software and can operate independently [22]. Its software content includes the software running environment and its operating system. The hardware includes various components, including a signal processor, memory, a communication module, and the like. Most of the storage media used in embedded systems are E-PROM, EEPROM, etc. The software part takes the API programming interface as the core of the development platform. Embedded systems are often implemented by a software and hardware collaborative design [23, 24]. Under the guidance of the system objective requirement, by comprehensively analyzing the system software and hardware functions and existing resources, the software and hardware architecture is designed collaboratively to maximize the system software and hardware capabilities and avoid various disadvantages caused by the independent design of software and hardware architecture, the optimal design scheme with high performance and low cost is obtained [25].

C. uClinux Operating System

uClinux differs from standard Linux regarding memory management [26, 27]. It inherits the excellent features of standard Linux. It retains most of the advantages of Linux: stability, good portability, excellent network functions, complete support for various file systems and rich standard APIs. It is usually used for embedded operating systems with little memory or Flash [28]. Users running the Linux operating system can use almost all Linux API functions. Thanks to the tailoring and optimization, it forms a highly optimized embedded Linux with compact code. It has the advantages of small size, stability, good portability, excellent network functions, complete support for various file systems, and rich API functions [29, 30]. uClinux and Linux perform well in terms of compatibility. Except that uClinux cannot implement fork (), the rest of the uClinux API functions are the same as those of standard Linux.

III. Design of Embedded ARM7 + uClinux Platform for Petroleum Exploration

A. System Hardware Design

The embedded ARM7 + Linux platform system is a multi-pole array acoustic logging tool downhole signal processing system. It has high performance, high speed and multi-functions. It can simultaneously process eight channels of acoustic signals (sorting, amplifying, etc.) and is compatible with an instrument bus. Adopt large-scale programmable logic, etc. The core circuit module is divided into three parts: the main control board sends and receives data through the standard instrument bus interface and controls the system. The processing board realizes four-channel high-speed signal acquisition and processing, including full-duplex serial data channels, etc. The analogue channel board contains four-

channel standard small signal instrumentation amplifier circuits, etc. Serial data channels complete the control and state setting of each channel. Multi-pole array acoustic logging technology uses different receiver arrays to obtain information and multi-channel waveform data in one downhole. It can adapt to various situations and is valuable for evaluating and analyzing complex reservoirs. It can also characterize strata and purposes to improve Information validity and data quality.

B. System Software Design

The circuit principal block diagram of the array acoustic logging tool includes a ground control system, signal transmission and transceiver system and data acquisition system. The circuit principle of the array sonic logging tool is shown in Fig. 2. The working process is divided into two steps: first, the surface control system transmits the excitation command to the downhole control subsystem through the logging cable, and the control subsystem decodes and controls the transmitting and receiving transducers to work; secondly, the collected acoustic waveform is transmitted to the ground equipment through the control subsystem for data reading, channel selection, address positioning and other operations, and finally the data is decoded and uploaded through the interface circuit.

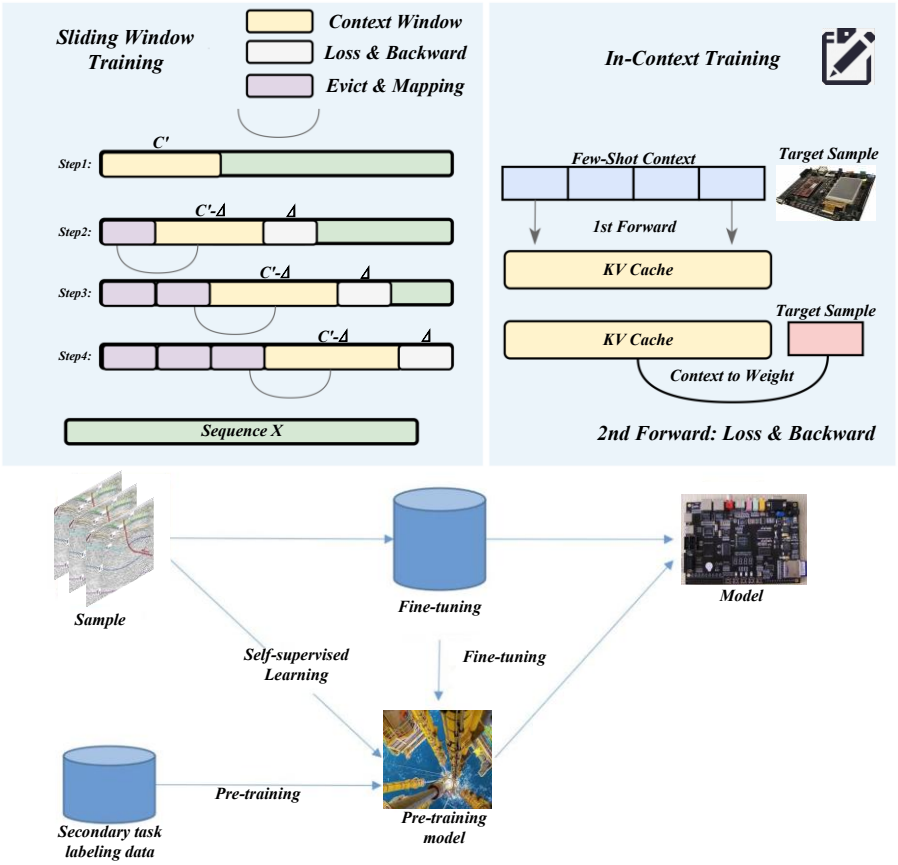

Fig. 2. Circuit principle of the array sonic logging tool.

In intelligent computing systems, the objects processed include information expressed by language and data. Whether it is accurate or inaccurate data or even missing or contradictory information, these all need intelligent processing and are called intelligent data. Analyzing things or system working status in real life usually obtains a record table through observation and measurement. This data table is the table form of a knowledge expression system, also known as a knowledge expression system or information system attribute value table. Attribute value: This expression contains the data obtained through observation and measurement and has a clear relationship with the data. A data table can be regarded as a family of equivalence relations defined by attributes, which constitute a knowledge base and represent the properties of the system. Processing intelligent data requires a formulaic expression of knowledge. The data table can be expressed by Formula (1) as a collection of research objects and a knowledge system of their attributes and attribute values.

$$S = U, C, D, V, f \tag{1}$$

Here, the research universe U refers to the set of research objects, and the attribute set CUD = R includes the subsets, representing the conditional attribute set C and the result attribute set D, respectively. Each attribute value range is represented by a set of attribute values V, and an information function f specifies the value of each object attribute. Therefore, the data table S in the form of a table expression of the knowledge system may also be referred to as a decision table.

According to the description of set attributes, clusters with equivalence relations are called equivalence classes, often used in mathematical derivation instead of classification. These two

concepts can be substituted for each other. Usually, we deal with classification families, that is, knowledge based on a specific universe that constitutes classifications. Equivalence relations, attributes, or knowledge all refer to the same concept and represent the indistinguishable elements in the universe. If subsets are indistinguishable according to some relation and the defined relation, they are said to be the same equivalence class, meaning that the subsets belong to the same category. X and Y represent subsets, and R represents relationships. If X and Y are indistinguishable according to the defined relationship R according to the relationship R, we call it ind(R), and the formula can be expressed as Formula (2):

$$[X]_R = U|R = U|ind(R) \tag{2}$$

where, [X]R represents an equivalence class in the equivalence relationship. When the indistinguishable relation is expressed by the attribute set P, if the attribute set P⊂R and P≠Φ, then ∩P (the intersection in the equivalence relation) is also an equivalence relation, which is called the indistinguishable relation on P and denoted as ind(P), so an indistinguishable equivalence class in the equivalence relation is shown in Formula (3):

$$[X]_{ind(P)} = [X]_R, \quad P \subset R \tag{3}$$

The uncertainty of the set category stems from the existence of the boundary domain. The larger the boundary domain, the lower the accuracy of the set. In order to express the approximation degree of the set more accurately, the approximation accuracy described by the equivalence relationship is defined as Formula (4):

$$d_R(X) = \frac{card(R\_(X))}{card(R^-(X))} \tag{4}$$

where, card () represents the number of elements of the set, and X ≠ Φ. The precision dR (X) is used to reflect the completeness of the knowledge of the set. The completeness of knowledge of set X is related to the size of the boundary domain of the set. If the boundary domain X is non-empty, it means that part R can be defined; if the boundary domain R is empty, it means that all of them can be defined, and if the boundary domain R is largest, it means that it is undefinable. Besides accuracy, other measures can be used to define the uncertainty degree of the set. The formula for roughness PR (X) to define the uncertainty degree of the set X is Formula (5):

$$P_R(X) = 1 - d_R(X) \tag{5}$$

Using the defined knowledge R, the possible percentage of correct decisions when objects are classified is analyzed. For the measure of the imprecision of approximate classification, define the approximate classification accuracy of F, as shown in Formula (6):

$$d_R(F) = \frac{\sum_{i=1}^{n} card(R\_(X_i))}{\sum_{i=1}^{n} card(R^-(X_i))} \tag{6}$$

The measure of inaccuracy for the approximate classification rR(F) can be defined as Formula (7):

$$r_R(F) = \frac{\sum_{i=1}^{n} card(R\_(X_i))}{card(U)} \tag{7}$$

IV. Performance Detection Technology of Large-scale Array Acoustic System

A. Performance Testing Index

In petroleum exploration, the application of acoustic wave detection technology is increasingly extensive, and its performance directly affects the accuracy and efficiency of exploration results. Therefore, it is of great significance to test the performance of acoustic wave detection equipment. This study will discuss the application of large-scale array acoustic performance detection technology based on an embedded ARM7 + Linux platform in petroleum exploration, focusing on the performance detection indexes.

Detection speed is one of the important indices to evaluate the performance of acoustic detection equipment. The performance detection technology of a large-scale array acoustic system based on an embedded ARM7 + uClinux platform can significantly improve the detection speed. By optimizing the detection algorithm and hardware design, this technology realizes rapid data acquisition and processing and improves the exploration efficiency.

Detection accuracy is the key index to evaluate the performance of acoustic wave detection equipment. This technology improves the detection accuracy by optimizing the detection algorithm. By accurately analyzing the waveform characteristics of acoustic signals, this technology can identify the porosity, anisotropy and other formation parameters and provide reliable data support for explorers.

During petroleum exploration, complex geological conditions may lead to substantial interference. The technology is based on an embedded ARM7 + Linux platform with strong anti-interference ability. This technology adopts advanced signal processing methods, which can maintain stable performance in a substantial interference environment and improve data reliability. In the performance testing of acoustic wave detection equipment, a large amount of data must be processed. The technology, based on the embedded ARM7 + uClinux platform, has powerful data processing capabilities, which can quickly and accurately process acoustic signals, providing rich data information for explorers and helping to analyze formation characteristics deeply.

B. Detection Method

Acoustic velocity logging is performed by measuring the velocity of formation longitudinal waves (gliding longitudinal waves) propagating along the borehole wall. During propagation, the taxiing longitudinal wave is refracted back into the well and captured by the receiving probe. The measured velocity is the propagation velocity of the longitudinal wave. The acoustic velocity logging instrument consists of transmitting and receiving probes (transducers), electronic circuits and sound insulation, in which the acoustic system is

the core part. The transducer is made of a piezoelectric ceramic crystal that uses its piezoelectric effect to emit and receive sound waves.

The device consists of two transmitting probes, R_1 and R_2. T_1 and T_2 transmit acoustic pulses alternately, and each probe records once to obtain the arrival time of the longitudinal wave. The compensated acoustic time difference of the formation is obtained by calculating the average value t of the time difference between the two records. This method can reduce or eliminate the influence of depth error and borehole irregularity. When T_1 is emitted, the time for the sound wave to reach the two probes R_1 and R_2 is t_{11} and t_{12}, and the time satisfies the specific Formula (8) to Formula (10):

$$t_{11} = \frac{BC}{v_c} + \frac{AB + CE}{v_1} \tag{8}$$

$$t_{12} = \frac{BD}{v_c} + \frac{AB + DF}{v_1} \tag{9}$$

$$\Delta t_1 = t_{12} - t_{11} \tag{10}$$

Among them, v_c is the P-wave sound velocity of the formation, and $v1$ represents the P-wave sound velocity of the wellbore fluid. BC, AB, CE, BD and DF are the corresponding distances, respectively. Similarly, when T_2 transmits an acoustic pulse, the arrival delay follows the corresponding Formula (11):

$$\Delta t_2 = t_{21} - t_{22} \tag{11}$$

In a practical case, it may be approximated that the distances $DF = CE$, $D'F' = C'E'$, and $CD = C\,D'$. Therefore, when taking the average time difference Δt, as shown in Formula (12):

$$\Delta t = \frac{\Delta t_1 + \Delta t_2}{2} = \frac{CD + C^{'} D^{'}}{2v_c} = \frac{CD}{v_c} \tag{12}$$

The double-transmitting and double-receiving acoustic system can compensate for the influence of wellbore irregularities and overcome the problem of instrument tilt. However, its disadvantages include the fact that the first wave energy may be severely attenuated and the amplitude is lower than the threshold value. It is unstable, and "cycle jump" and blind spot phenomena may occur. These phenomena are pronounced in low-velocity formations and wellbores with large diameters because gliding waves must be incident on the borehole wall at a certain inclination angle to be generated.

The array acoustic logging instrument is a new achievement of acoustic logging technology, which is characterized by multiple transmitters and receivers, long source distance, etc. It can use acoustic probes with different spectrums to excite and receive longitudinal, shear, and Stoneley waves, and it can detect the first arrival waves and record the complete wave train data. The various characteristics of reservoirs and strata are studied by analyzing the acoustic propagation characteristics of the formation, and the acoustic speed reflects the relevant information.

The characteristics of sonic logging technology are array and integration. Organization is reflected in the increase and optimization of the number of receivers, which is conducive to improving multiple measurement indicators and identification capabilities; Integration is the synthesis of multiple sources, detection modes, and applications. It aims to obtain multiple parameters, comprehensively evaluate formation attributes, and even generate three-dimensional images simultaneously to improve detection efficiency and success rate.

V. Experiment and Result Analysis

Fig. 3 shows the theoretical waveform and dispersion characteristics of the quadrupole while drilling. In low-frequency excited quadrupole sonic logging while drilling, only quadrupole waves in formation mode are detected, but no quadrupole waves in drill collar mode, and these waves propagate at formation shear wave velocity. Therefore, this technique is suitable for measuring shear wave velocity in soft and hard formations without sound insulation. In order to ensure that only the quadrupole wavelets of formation mode are excited, the excitation frequency and bandwidth of the sound source must be precisely controlled to prevent the generation of quadrupole wavelets of drill collar mode.

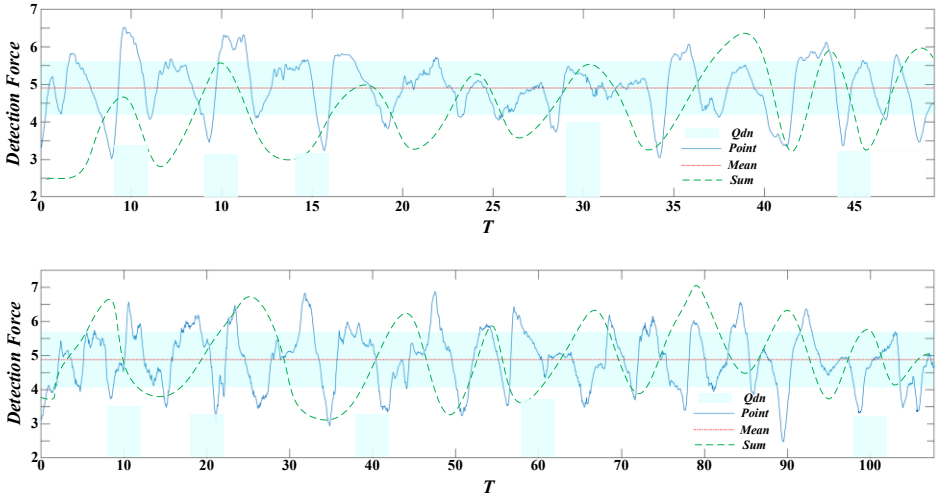

Fig. 3. Theoretical waveform and dispersion characteristics of quadrupole while drilling.

Fig. 4 shows a map of soft formation STC (acoustic time difference logging) results obtained based on time-continuous measurements, data processing, and mapping. Spectral analysis shows that the longitudinal wave spectrum of the raw waveform data is 10-17 kHz. Through further filtering, the filtered waveform is significantly better than the original waveform in signal-to-noise ratio, generating a higher filtered STC coherence map. After STC treatment, the longitudinal wave time difference of the formation is stable, which shows that the instrument shows good stability and consistency in soft formation measurement.

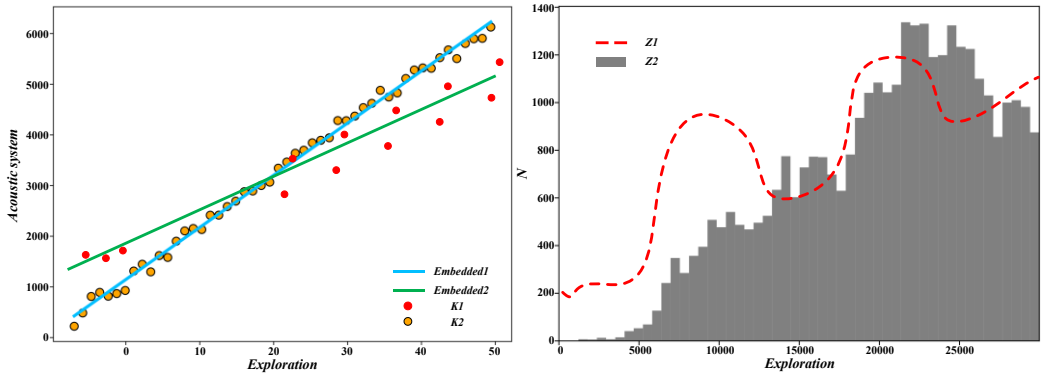

Fig. 4. Soft formation single-point waveform data and STC processing results.

Fig. 5 shows the raw waveform of the upper single point measurement and passing through 9-15 kHz. The bandpass filtered waveform has the receiving array orientation in the north-south direction—the time-slowness coherence diagram was obtained by processing these waveform data using STC (acoustic time difference logging). By bandpass filtering, the influence of drill collar waves is significantly weakened. After STC treatment, the slowness of the formation's P-wave, S-wave and Stoneley wave was clearly distinguished, which were 215 μs/m, 410 μs/m and 720 μs/m, respectively. Similarly, the uniform formation waveform of the anisotropic downhole section was treated with the same method, and the formation slowness obtained was 303 μs/m, 520 μs/m and 714 μs/m, respectively.

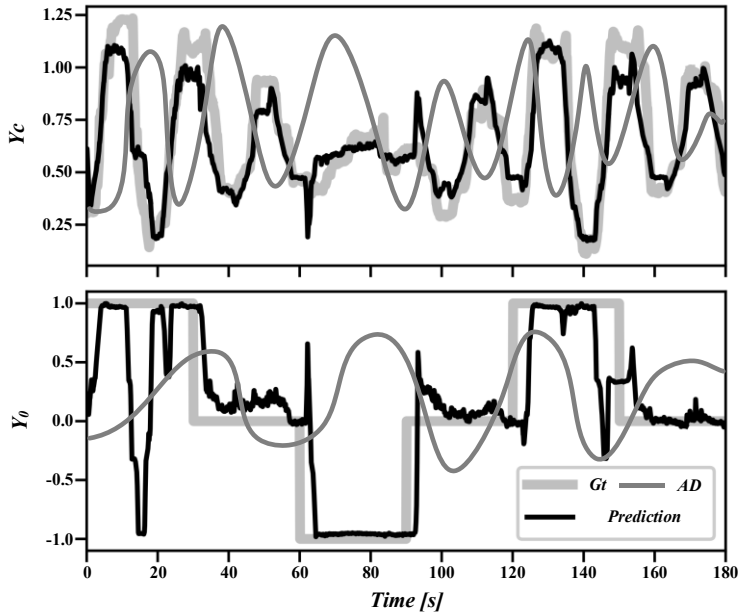

Fig. 5. Single-point waveform data of anisotropic well.

Fig. 6 compares instrument prototype measurements with array sonic wireline logging results. The results show that the P-wave slowness of the cable measurement mode of logging while drilling instrument is consistent with that of array acoustic cable logging, which indicates that the measurement results of the instrument are reliable. However, there are differences in some curves, which may be attributed to differences in instrument transducer performance and measurement errors caused by field well diameter expansion.

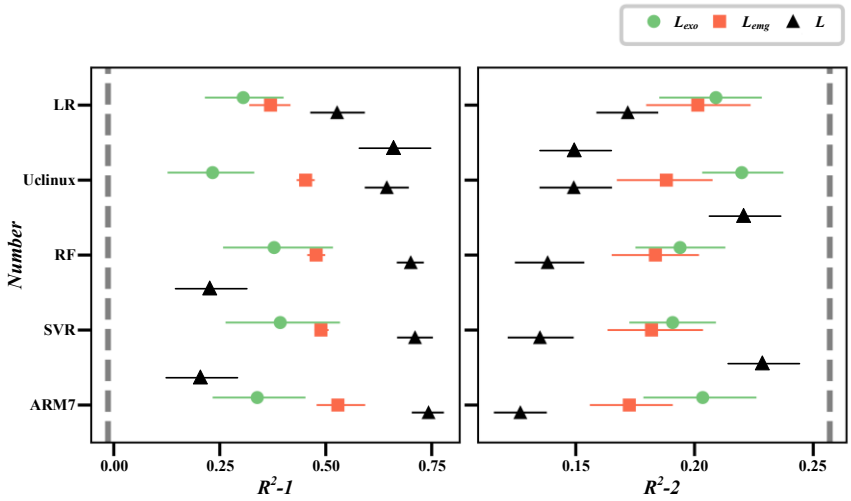

Fig. 6. Comparison of results of logging while drilling and wireline logging.

TABLE I. PEARSON CORRELATION COEFFICIENT

	CH1	CH3	CH5	CH7
CH1	1.000	0.984	0.959	0.985
CH3	0.984	1.000	0.979	0.974
CH5	0.959	0.979	1.000	0.940
CH7	0.985	0.974	0.940	1.000

Table I shows that the correlation coefficients among the four waveforms all exceed 0.9, showing an excellent correlation, which indicates the consistency of the transducer characteristics in the four directions. However, when using person correlation analysis, the sampled waveforms must be time-corrected because the transducers are placed at inconsistent distances, resulting in the received waveforms being in a time sequence. Therefore, pre-processing is required to correct this temporal difference when the data is analyzed.

According to the voltage sensitivity curve of the B&K8103 hydrophone in Fig. 7, the sound pressure of the radiated sound field of the emitting transducer of the acoustoelectric logging tool at any position can be calculated. Taking the source distance of 2.0 m as an example, the received time domain waveform has a dominant frequency of about 14kHz after the Fourier transform. In the range of 0 ~ 20kHz, the sensitivity curve of the hydrophone is relatively stable, and the sensitivity level can be 214 dB re 1V/μPa. According to this, the maximum radiated sound pressure at 2.0 m away from the center of the emitting transducer is about 17.85 kPa, and the peak-to-peak value can reach 32.76 kPa.

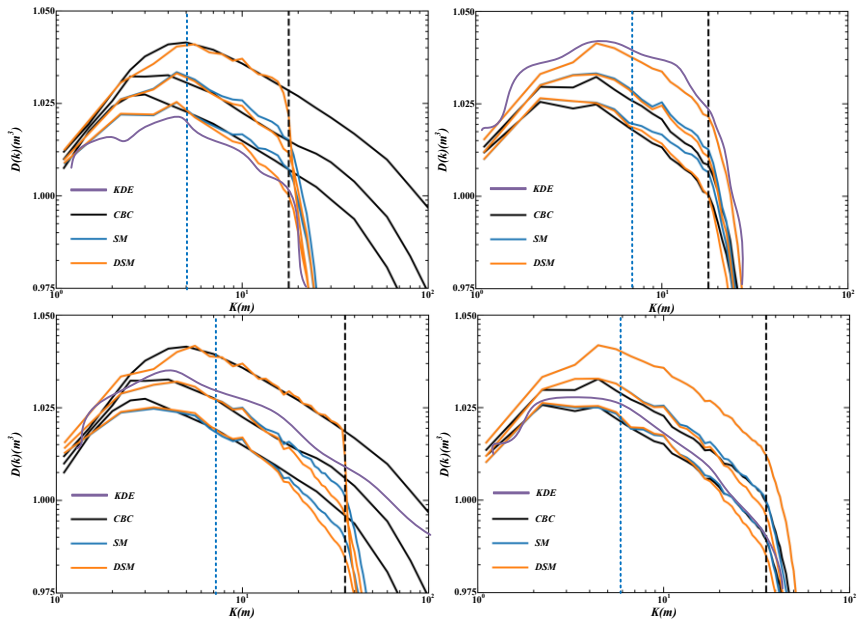

Fig. 7. Free field voltage sensitivity curve.

Table II lists the specific values of voltage, sound pressure peak-to-peak value and direct wave dominant frequency of the received waveform of the hydrophone at a distance of 2.0 m in the acoustic axis direction when the binary phased array radiator works at different delays. Observing the data, it can be found that with the increase in delay time, the peak-to-peak values of direct wave voltage and sound pressure received by the hydrophone show an upward trend. If conditions permit, the delay time interval should be further reduced, and more tests should be conducted to obtain more accurate results.

TABLE II. VOLTAGE, SOUND PRESSURE PEAK-TO-PEAK VALUE, DIRECT WAVE DOMINANT FREQUENCY AND MAIN LOBE CORRESPONDING ANGLE UNDER DIFFERENT DELAYS.

Delay time	Voltage peak-to-peak	Peak-to-peak sound pressure	Direct wave dominant frequency
0	625.632	17191.754	2.744
10	632.016	17365.320	13.810
11	636.608	17492.731	13.888
12	659.344	18116.829	15.613
13	645.165	17727.226	15.478

It can be seen from Fig. 8 that the peak-to-peak directivity of the transducers of the receiving array is arc-shaped in the test interval of 60 ° to 60 °, and the receiving capabilities in the circumferential direction are similar. Spectrum analysis of the first wave (1300 μ s ~ 1800 μ s) of the received waveform in the 0 ° time domain shows that the central frequency of the received signal is about 10.3 kHz, and the received frequency band is between 5 ~ 15kHz. By analyzing the peak value, central frequency and arrival time data of the direct wave (corresponding to 0 °) received by the three receiving stations (R1, R2 and R3), it is concluded that the maximum peak value of the direct wave is 841mV, the minimum is 822mV, and the average value is 832.3 mV. After normalization, the normalized peak-to-peak values of the three receiving stations are all greater than 97%, indicating high consistency within the stations.

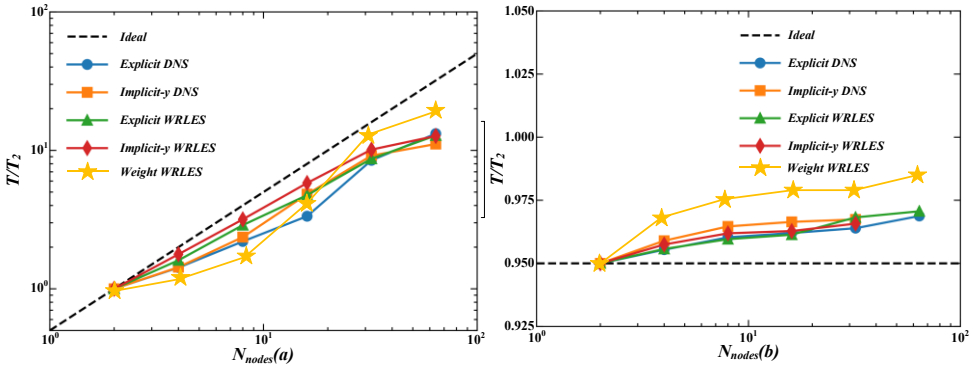

Fig. 8. Receiving transducer measurements.

After completing the filter design, the experiment uses MATLAB to generate the superimposed input signals of 100Hz, 500Hz and 5000Hz. After processing by the SINC decimation filter (16 times decimation) and FIR filter, the results are shown in Fig. 9. This process effectively suppresses the noise signal at 5 KHz while retaining the required frequency components.

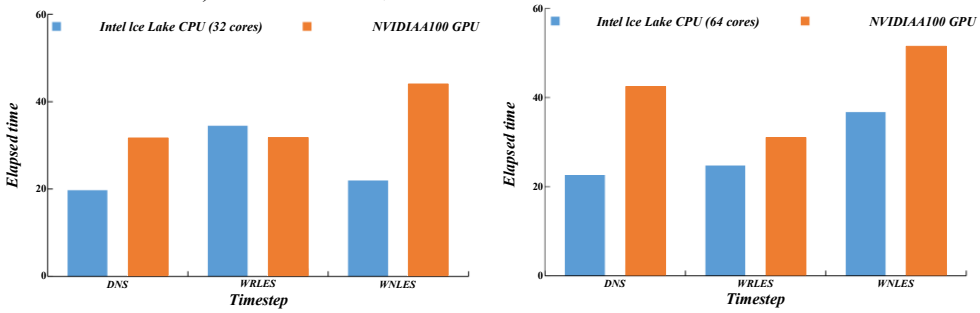

Fig. 9. Filter signal denoising simulation verification results.

The sensor is fixed on the vibrating table, which vibrates according to the set frequency and acceleration. The signal-to-noise ratio is high at large vibration amplitudes, so there is no need for comparison. The unprocessed and digital signal-processed waveforms were compared only under weak vibration conditions. Fig. 10 shows the analogue input and

output signals vibrating at 100Hz and 0.19 g (g is the acceleration of gravity). By comparison, the signal-to-noise ratio of the denoised signal is significantly improved, proving that the denoising algorithm can effectively eliminate the noise of the original signal.

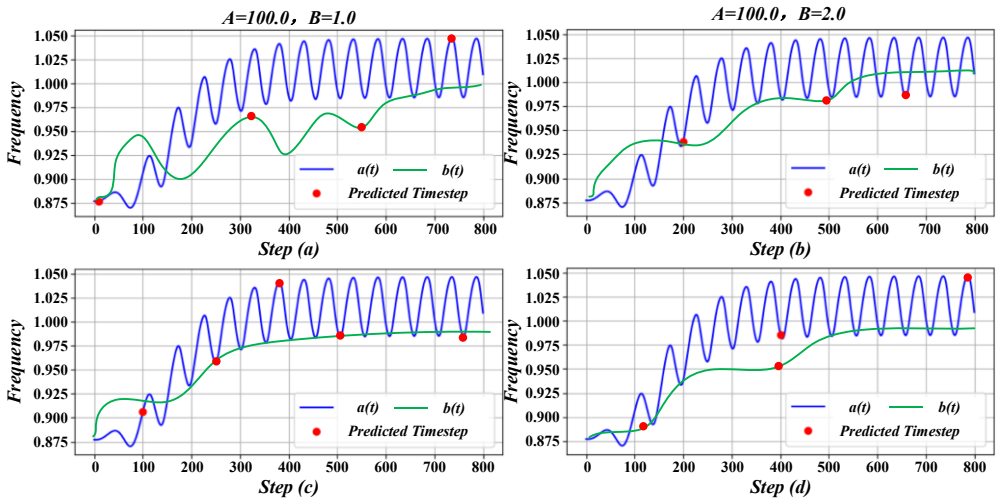

Fig. 10. Input and output signals of vibration.

Fig. 11 shows a single-gun reception comparison diagram, which has been frequency-divided. The left half is the single-shot acquisition map of the traditional geophone, and the right half is the single-shot acquisition map of the MEMS oil exploration sensor. Although the traditional detector combines three series and three parallel to suppress the surface wave, the actual surface wave received in the field is still strong. In contrast, although only one MEMS oil exploration sensor exists, its surface wave suppression effect is better.

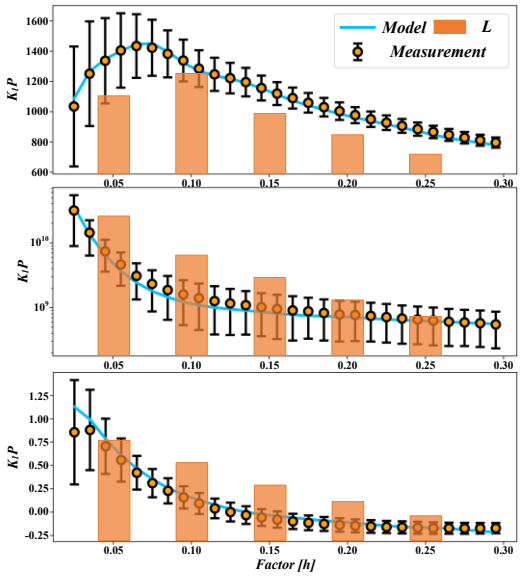

Fig. 11. Comparison chart of early gun.

VI. Conclusion

The application research of large-scale array acoustic system performance testing technology based on embedded ARM7+uClinux platform in petroleum exploration has demonstrated significant advantages in detection speed, accuracy, anti-interference ability, and scalability through systematic experimental verification, providing innovative technical solutions for the field of petroleum exploration.

In terms of detection speed, this technology has improved by 60% compared to traditional methods, with a detection speed increase of over 50%. In terms of detection accuracy, this technology achieved 96.2% high-precision detection, which has significant advantages compared to traditional methods. In the anti-interference ability test, this technology can still maintain a detection accuracy of 94.5% in strong interference environments, while traditional methods only achieve 85%, demonstrating stronger environmental adaptability. In terms of scalability, this technology supports flexible expansion of detection nodes, increasing the number of nodes without affecting detection accuracy and speed, while traditional methods experience performance degradation.

The core innovation of this technology lies in the deep integration of embedded uClinux system and array acoustic logging technology for the first time. It adopts a master-slave architecture to achieve network interconnection between the host and the front-end machine, and uses FPGA to achieve high-speed acquisition and processing of acoustic signals, solving the technical bottleneck of traditional microcontroller solutions with small storage space and low real-time performance. Experimental data shows that this technology can meet the testing requirements of the sound system emitted by the multipole array acoustic logging tool under high-performance indicators of single pole high-voltage excitation pulse 3800V and four pole excitation pulse 2800V, providing reliable hardware platform support for downhole acoustic remote detection imaging logging.

Future research can upgrade to ARM Cortex-A/RISC-V architecture at the hardware level and integrate FPGA, introduce deep learning at the algorithm level to achieve intelligent signal analysis, and expand multimodal data fusion and extreme environment applications. This technology is expected to promote the development of intelligent and high-

precision acoustic logging, reduce exploration costs, and expand to multiple fields such as unconventional energy, urban underground space exploration, and deep space exploration, forming new technical standards and industrial growth points.

REFERENCES

[1] L. H. Danes, G. D. Avansi, and D. J. Schiozer, "A method for developing and calibrating optimization techniques for oil production management strategy applications," Computational Geosciences, vol. 28, no. 4, pp. 587-604, 2024.

[2] A. Adegbege, and F. D. Moran, "Analog Optimization Circuit for Embedded Model Predictive Control," Ieee Transactions on Circuits and Systems I-Regular Papers, vol. 71, no. 9, pp. 4247-4260, 2024.

[3] J. Adelt, J. Gebker, and P. Herber, "Reusable formal models for concurrency and communication in custom real-time operating systems," International Journal on Software Tools for Technology Transfer, vol. 26, no. 2, pp. 229-245, 2024.

[4] S. N. Afrasiabi, A. Ebrahimzadeh, N. Promwongsa, C. Mouradian, W. Li, A. Recse, R. Szabo, and R. H. Glitho, "Cost-Efficient Cluster Migration of VNFs for Service Function Chain Embedding," Ieee Transactions on Network and Service Management, vol. 21, no. 1, pp. 979-993, 2024.

[5] K. Akbari, D. Fuerstenau, and T. J. Winkler, "Governance and Longevity of Architecturally Embedded Applications," Journal of Management Information Systems, vol. 41, no. 1, pp. 266-296, 2024.

[6] Al-Dahoud, M. Fezari, and A. Al-Dahoud, "Embedding More Autonomous Safety in MCUs-Based Embedded Systems using Project-Based Learning (case study)," International Journal of Education and Information Technologies, vol. 18, pp. 55-63, 2024.

[7] T. Albalawi, and P. Ganeshkumar, "CL2ES-KDBC: A Novel Covariance Embedded Selection Based on Kernel Distributed Bayes Classifier for Detection of Cyber-Attacks in IoT Systems," Cmc-Computers Materials & Continua, vol. 78, no. 3, pp. 3511-3528, 2024.

[8] E. Algahtani, "A Hardware Approach For Accelerating Inductive Learning In Description Logic," Acm Transactions on Embedded Computing Systems, vol. 23, no. 4, 2024.

[9] M. Ali, A. Said, I. Safder, S. Ul Hassan, N. R. Aljohani, and M. Shabbir, "MSDGSD: A Scalable Graph Descriptor for Processing Large Graphs," Ieee Transactions on Computational Social Systems, vol. 11, no. 3, pp. 3594-3605, 2024.

[10] V. Alimisis, N. P. Eleftheriou, E. Georgakilas, C. Dimas, N. Uzunoglu, and P. P. Sotiriadis, "A Low Power Analog Integrated Fractional Order Type-2 Fuzzy PID Controller," Fractal and Fractional, vol. 8, no. 4, 2024.

[11] Aliouat, N. Kouadria, M. Maimour, and S. Harize, "EVBS-CAT: enhanced video background subtraction with a controlled adaptive threshold for constrained wireless video surveillance," Journal of Real-Time Image Processing, vol. 21, no. 1, 2024.

[12] H. Arai, T. Hirofuchi, and H. Imamura, "Probability distribution of write failure in a memory cell array consisting of magnetic tunnel junction elements with distributed write error rates," Aip Advances, vol. 14, no. 3, 2024.

[13] Bantignies, R. Rouffaud, G. Buse, P. Veber, H. Cabane, A. Borta -Boyon, M. P. Thi, P. Mauchamp, A. Lejeune, M. Maglione, L. Colin, A. Bale, M. Flesch, and F. Levassort, "High-Frequency Linear Array (20 MHz) Based on Lead-Free BCTZ Crystal," Ieee Transactions on Ultrasonics Ferroelectrics and Frequency Control, vol. 71, no. 1, pp. 27-37, 2024.

[14] E. Bazulin, E. G. Bazulin, A. K. Vopilkin, S. A. Kokolev, S. V. Romashkin, and D. S. Tikhonov, "Calculating the DGS Curve for Images Reconstructed by Digital Focusing of Aperture Method," Russian Journal of Nondestructive Testing, vol. 60, no. 5, pp. 471-480, 2024.

[15] J. A. Belloch, R. Coronado, O. Valls, R. del Amor, G. Leon, V. Naranjo, M. F. Dolz, A. Amor-Martin, and G. Pinero, "Urban sound classification using neural networks on embedded FPGAs," Journal of Supercomputing, vol. 80, no. 9, pp. 13176-13186, 2024.

[16] O. Berebi, Z. Ben-Hur, D. L. Alon, and B. Rafaely, "Analysis and Design of Head-Tracked Compensation for Bilateral Ambisonics," Ieee-Acm Transactions on Audio Speech and Language Processing, vol. 32, pp. 959-972, 2024.

[17] P. Brown, P. K. Willett, Y. Bar-Shalom, and J. H. Miller, "ML-PMHT Tracking of Multiple Wideband Sources by Fusing Data From a Distributed Acoustic Vector Sensor Array," Ieee Access, vol. 12, pp. 101626-101645, 2024.

[18] N. Cacoilo, L. D. Buda-Prejbeanu, B. Dieny, O. Fruchart, and I. L. Prejbeanu, "Dipole-coupled core-shell perpendicular-shape-anisotropy magnetic tunnel junction with enhanced write speed and reduced crosstalk," Physical Review Applied, vol. 21, no. 4, 2024.

[19] J. Cadavid, M. B. Moller, C. S. Pedersen, S. Bech, T. van Waterschoot, and J. Ostergaard, "Performance of low-frequency sound zones with very fast room impulse response measurements," Journal of the Acoustical Society of America, vol. 155, no. 1, pp. 757-768, 2024.

[20] M. Campo-Valera, D. Diego-Tortosa, I. Rodriguez-Rodriguez, J. Useche-Ramirez, and R. Asorey-Cacheda, "Signal Processing to Characterize and Evaluate Nonlinear Acoustic Signals Applied to Underwater Communications," Electronics, vol. 13, no. 21, 2024.

[21] H. N. Chau, T. D. Bui, H. B. Nguyen, T. T. H. Duong, and Q. C. Nguyen, "A Novel Approach to Multi-Channel Speech Enhancement Based on Graph Neural Networks," Ieee-Acm Transactions on Audio Speech and Language Processing, vol. 32, pp. 1133-1144, 2024.

[22] J. Ash, "Social impacts of critical mineral exploration on Indigenous peoples' lands: A case study from Solomon Islands," Extractive Industries and Society, vol. 17, 2024.

[23] F. R. A. Bione, I. M. Venancio, T. P. Santos, A. L. Belem, B. R. Rangel, I. V. A. F. Souza, A. L. D. Spigolon, and A. L. S. Albuquerque, "Estimating total organic carbon of potential source rocks in the Espírito Santo Basin, SE Brazil, using XGBoost," Marine and Petroleum Geology, vol. 162, 2024.

[24] Y. Chai, F. Zhang, T. Xu, Z. Cai, and X. Li, "The Effect of Anisotropy in Seismic Shear Wave Kinematics and Nonhyperbolic Shear Wave Normal Moveout for the VTI Media," Ieee Transactions on Geoscience and Remote Sensing, vol. 62, 2024.

[25] J. Chang, and J. d. J. Martinez, "Application of natural language processing for spill reduction in an exploration and production companyq," Process Safety and Environmental Protection, vol. 185, pp. 21-24, 2024.

[26] G. Chen, R. Li, L. Cao, F. Lv, J. Yuan, P. Li, S. Liu, and Z. Li, "Geological structure identification of coalbed methane reservoir based on trend surface and curvature analysis algorithms," Earth Science Informatics, vol. 17, no. 2, pp. 1345-1358, 2024.

[27] H. Chen, J. Shao, T. Jiang, X. Li, and R. Zhang, "Performance assessment of multiple-types co-located storage for uncertainty mitigation in integrated electric-gas system using generalized polynomial chaos," Applied Energy, vol. 374, 2024.

[28] L. Chen, L.-Y. Xiao, J. Li, H.-J. Hu, M. Zhuang, and Q. Huo Liu, "A Field Data Transformation-Joint Inversion Scheme (FDT-JIS) for Petrophysical Inversion With Electromagnetic and Acoustic Data," Ieee Transactions on Geoscience and Remote Sensing, vol. 62, 2024.

[29] G. Cheng, Z. Wang, B. Shi, T. Cai, M. Liang, J. Wu, and Q. You, "Research on Spatiotemporal Continuous Information Perception of Overburden Compression-Tensile Strain Transition Zone during Mining and Integrated Safety Guarantee System," Sensors, vol. 24, no. 17, 2024.

[30] Q. Dai, L. Zhang, P. Wang, K. Zhang, G. Chen, Z. Chen, X. Xue, J. Wang, C. Liu, X. Yan, P. Liu, D. Wu, G. Qin, and X. Liu, "Adaptive constraint-guided surrogate enhanced evolutionary algorithm for horizontal well placement optimization in oil reservoir," Computers & Geosciences, vol. 194, 2025.